

Topological delocalization of two-dimensional massless Dirac fermions

Kentaro Nomura,¹ Mikito Koshino,² and Shinsei Ryu³

¹ *Department of Physics, Tohoku University, Sendai, 980-8578, Japan*

² *Department of Physics, Tokyo Institute of Technology,
2-12-1 Ookayama, Meguro-ku, Tokyo 152-8551, Japan*

³ *Kavli Institute for Theoretical Physics, University of California, Santa Barbara, CA 93106, USA*

(Dated: November 1, 2018)

The beta function of a two-dimensional massless Dirac Hamiltonian subject to a random scalar potential, which, e.g., underlies theoretical descriptions of graphene, is computed numerically. Although it belongs to, from a symmetry standpoint, the two-dimensional symplectic class, the beta function monotonically increases with decreasing conductance. We also provide an argument based on the spectral flows under twisting boundary conditions, which shows that none of states of the massless Dirac Hamiltonian can be localized.

PACS numbers: 72.10.-d,73.21.-b,73.50.Fq

The single parameter scaling theory of Anderson localization [1] predicts that the quantum transport of non-interacting disordered conductors is characterized by the beta function

$$\beta(g) = \frac{d \ln g}{d \ln L}, \quad (1)$$

which encodes the variation of the dimensionless conductance g with respect to the system size L . Once the value of the conductance at some length scale is known, the quantum transport at all length scales is constructed. [2] The property of the beta function depends on the dimensionality, and also on the symmetry class of the microscopic Hamiltonian, such as spin rotation and time-reversal (TR) symmetries. [3] In addition, the topological nature of wavefunctions also has a significant effect on quantum transport.

In this paper, we discuss the problem of Anderson localization for the two-dimensional (2D) two-component Dirac Hamiltonian subject to a random scalar potential,

$$\mathcal{H} = -i\hbar v_F \boldsymbol{\sigma} \cdot \nabla + V(\mathbf{r}). \quad (2)$$

Here, $\mathbf{r} \in \mathbb{R}^2$, $\sigma_{x,y,z}$ denote the standard Pauli matrices, and v_F the constant velocity. The details of the random scalar potential $V(\mathbf{r})$ will be specified later.

The random Dirac Hamiltonian (2) is of direct relevance to the quantum transport of disordered graphene. [4] Although the band structure of clean graphene has two flavors (valleys) of two-component Dirac fermions, the intervalley scattering is rather weak since spatial profile of disorder in graphene is supposed to be smooth on an atomic scale. [5, 6] A two-component single-flavor Dirac fermion can be realized, without doubling, on a surface of a three-dimensional \mathbb{Z}_2 topological insulator. [7, 8, 9]

The properties of the eigen functions for the ideal Dirac Hamiltonian (Eq. (2) without V) are well-known: The degeneracy point in the momentum space serves as a

Dirac monopole for the Berry connection and wavefunctions in the momentum space pick up a π phase shift when transported around the Dirac cone. [10]

From the symmetry point of view, the random Hamiltonian (2) belongs to the symplectic symmetry class, as it possesses an “effective” TR symmetry

$$i\sigma_y \mathcal{H}^* (-i\sigma_y) = \mathcal{H}. \quad (3)$$

[11] The beta function of the 2D symplectic class shows the weak-antilocalization for large g , and there is a metal-insulator transition at $g^* \sim 1.4$. [12, 13, 14]

Although being a member of the symplectic symmetry class, there is growing evidence that the beta function of the random Dirac Hamiltonian (2) is qualitatively different from the conventional one for the 2D symplectic class: (i) Localization of non-relativistic electrons for strong disorder can be understood in a picture in which bound states localized at potential minima overlap with each other. However, a Dirac fermion cannot be trapped by a potential well irrespective of the well depth [15, 16], and hence is naively expected to have a strong tendency not to be insulating. This makes a physical picture for the strongly disordered regime of the Dirac fermions different from the conventional case, although physics of Anderson localization cannot fully be understood in terms of potential trapping. (ii) As observed by Ando *et al.*, the Berry phase π that is accumulated around the Dirac cone in the momentum space leads to a destructive interference between a back scattering process and its TR counterpart, leading to the complete absence of back scattering. [10] (iii) The non-linear sigma model (NL σ M, a field theory for diffusion modes) for the random Dirac Hamiltonian (2) has a \mathbb{Z}_2 topological term. [17, 18, 19] It has a little effect in the metallic regime, but should change the renormalization group flow in the strongly disordered regime. Ostrovsky *et al.* [18] conjectured the NL σ M with the topological term has three fixed points (metallic fixed point, metal-semi-metal transition, and semi-metal attractive fixed point). (iv) There are numerical studies

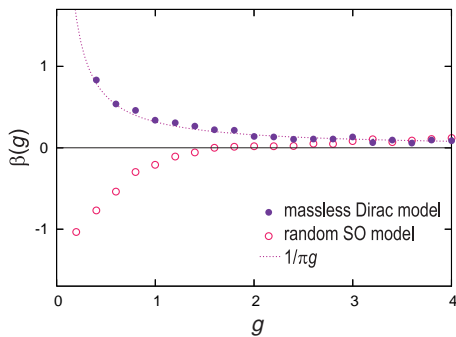


FIG. 1: (Color online) The beta functions of the random Dirac Hamiltonian (2) (closed circles) and the random spin-orbit model (6) (open circles). The broken line represents the one-loop beta function of the conventional 2D symplectic class, $\beta(g) \sim 1/\pi g$. [12]

that indicate the increase of the conductance with system size even for $g \lesssim 1.4$. [20, 21]

The purpose of this paper is to compute the beta function of (2) numerically, and compare it with conventional system of the 2D symplectic class. We find that the beta function of the Dirac model is always larger than or equal to zero, showing that all states are delocalized even in the strong disorder regime, in contrast to the conventional case. We also provide a spectral-flow argument that clearly shows that the localization of Dirac fermions is forbidden.

We compute the diagonal conductance (conductivity) of the random Dirac Hamiltonian (2) by evaluating the Kubo formula

$$g = -\frac{i2\pi\hbar^2}{L^2} \sum_{n,n'} \frac{f(E_n) - f(E_{n'})}{E_n - E_{n'}} \frac{\langle n|v_x|n'\rangle \langle n'|v_x|n\rangle}{E_n - E_{n'} + i\eta}, \quad (4)$$

where \mathbf{v} is the velocity operator, $\mathbf{v} = i[\mathcal{H}, \mathbf{r}]/\hbar = v_F \boldsymbol{\sigma}$, $f(E)$ is the Fermi-Dirac function at zero-temperature, η in the energy denominator is a smearing factor, and $|n\rangle$ denotes an eigenstate with energy E_n of the Dirac equation in the presence of the random potential.

The massless two-component Dirac equation cannot be regularized, without breaking the TR symmetry, by putting the system on a lattice. We thus work in the momentum space by introducing a hard cutoff at a sufficiently large momentum Λ . The eigenstates $\{|n\rangle\}$ and energies $\{E_n\}$ are then obtained by numerically diagonalizing the Dirac Hamiltonian with disorder in the momentum-pseudospin basis. Typically, we take $\Lambda \sim 20 \times 2\pi/L$, where about 2000 k -points are included. We assume that the disorder potential is sufficiently weak so that the level broadening caused by disorder around the Dirac point is much smaller than the cut-off energy $\propto \Lambda$.

The smearing factor η in the denominator of Eq. (4) accounts for the finite switch-on time of the electric field required for a dissipative current response. Physical ar-

guments suggest that η has to be at least as large as \hbar/T_L where T_L is the escape time from the system of interest. The escape time can be estimated from the Thouless energy $\langle \Delta E \rangle$ by the uncertainty relation $\langle \Delta E \rangle T_L \simeq \hbar$, where ΔE is the eigenvalue difference between periodic and antiperiodic boundary conditions and $\langle \rangle$ is the geometric mean over disorder realizations. [22, 23] Indeed, it is reported in Ref. [20] that g is reasonably insensitive to η when $\eta \simeq \langle \Delta E \rangle$.

We assume that the scalar potential disorder $V(\mathbf{r})$ is generated by randomly distributed impurities centered at \mathbf{R}_I , each of which contributes to $V(\mathbf{r})$ with a scattering potential $U(\mathbf{r} - \mathbf{R}_I)$,

$$V(\mathbf{r}) = \sum_{I=1}^{N_i} U(\mathbf{r} - \mathbf{R}_I). \quad (5)$$

We considered two types of scattering potentials $U(\mathbf{r})$: the Gaussian correlated potential, $U(\mathbf{q}) = u \exp(-q^2 l_0^2/2)$, and the Thomas-Fermi potential, $U(\mathbf{q}) = u/(q + l_0^{-1})$, where $U(\mathbf{q})$ is the Fourier transform of $U(\mathbf{r})$, u represents the disorder strength, and l_0 the range of the potential. Typically 5000 disorder configurations were used for averaging. The conductance was calculated for various sets of parameters, N_i , u , l_0 and filling (E_F); The number of scatterers N_i was 1-10 times as large as the maximum number of carriers at each size; The range of the potential was changed upto 1/30 of the minimal system size.

We note that typical length scales are hardly determined from naive considerations at the Dirac point ($E_F^{-1} \rightarrow \infty$). Indeed the mean free path at the Dirac point, estimated by the golden rule, diverges for uncorrelated short-range scattering ($l_0 \rightarrow 0$)[5], while it vanishes for long-range Coulomb scattering ($l_0 \rightarrow \infty$)[20]. Nevertheless we do not need the specific length scale since the beta function is defined as a logarithmic derivative in Eq. (1).

To compare our results with the conventional 2D symplectic class, we compute, by the same method, the beta function of the random spin-orbit (SO) coupling model given by

$$\begin{aligned} \mathcal{H} &= (-i\hbar\nabla)^2/2m + V(\mathbf{r}) + V_{\text{so}}, \\ V_{\text{so}} &= -\frac{1}{2}\{\lambda(\mathbf{r}), -i\nabla\} \times \boldsymbol{\sigma} \cdot \hat{\mathbf{z}}. \end{aligned} \quad (6)$$

Note that the velocity operator in this model is spin-dependent. We assume an uncorrelated short-range distribution for $\lambda(\mathbf{r})$ and $V(\mathbf{r})$.

Figure 1 shows the beta function of the Dirac model (filled circles) and the random SO coupling model (open circles). The latter agrees with the known behavior of the beta function of the 2D symplectic universality class: there is a metallic phase with weak anti-localization effect ($\beta(g) \sim 1/\pi g$) when g is large, whereas there is a localized phase for small g ; there is a metal-insulator transition at $g^* \sim 1.5$ that separates the two phases.

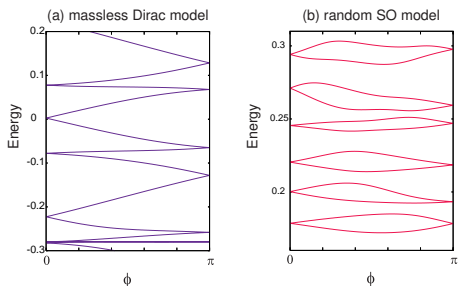


FIG. 2: (Color online) The evolution of energy spectra as a function of the twist angle ϕ for the random massless Dirac model (left) and the random spin-orbit model (right).

For large g , the beta function of the random Dirac model behaves similarly as that of the random SO model; this is as expected since when g is large, the \mathbb{Z}_2 topological effect in the NL σ M is small.

We observe that the single parameter scaling holds reasonably well in both models as shown in Fig. 1. [24] In a sharp contrast to the conventional case, the beta function of the Dirac model monotonically increases with decreasing g well below $g^* \sim 1.4$: A 2D massless Dirac fermion cannot be localized by a random scalar potential. [25] The numerical beta function of the Dirac model is well fitted by the one-loop beta function of the symplectic class even in the strongly disordered regime $g \lesssim 1$.

The absence of localization in the Dirac model can intuitively be understood by examining the spectral flow induced by twisting boundary conditions. Let us consider a finite and disordered system described by Eq. (2), and impose the boundary conditions in both x and y directions, with phase factors $\exp(i\phi_x)$ and $\exp(i\phi_y)$, respectively. For simplicity we set $\phi_y = 0$ and discuss the energy levels as a function of $\phi_x \equiv \phi$. The TR symmetry holds at $\phi = 0, \pi$, where $\exp(i\phi)$ is real, leading to the Kramers degeneracy. We assume the cutoff to be infinity (the effects of the finite cutoff will be discussed later). Fig. 2(a) shows an example of spectral flow obtained for the 2D Dirac model with a specific disorder configuration. An essential observation is that Kramers pairs always change their partners as the energy spectrum evolves from $\phi = 0$ to π ; if the energy eigenvalues $\{E_n\}$ are paired as $\dots, (E_n, E_{n+1}), (E_{n+2}, E_{n+3}), \dots$ at $\phi = 0$, then they are paired as $\dots, (E_{n-1}, E_n), (E_{n+1}, E_{n+2}), \dots$ at $\phi = \pi$. Here eigenvalues E_n are ordered in ascending order [26]. In contrast, the non-relativistic electron system with SO coupling has a different type of the ‘band-line topology’ as shown in Fig. 2(b); energy eigenvalues do not change their partners as the spectrum evolves from $\phi = 0$ to π .

We can find the origin of this topological structure in the ideal spectrum. In the absence of disorder, the Dirac model has a set of eigenvalues $E_{n_x, n_y, s}(\phi) = (2\pi/L)\hbar v_F s [(n_x + \phi)^2 + n_y^2]^{1/2}$, where $s = \pm 1$ and

$n_x, n_y \in \mathbb{Z}$. For example, two degenerate states at $\phi = 0$ with zero energy ($s = \pm 1$ and $n_x = n_y = 0$) become apart as ϕ increases and never stick together; each couples with other partners at $\phi = \pi$. As we introduce disorder, energy eigenvalues move around but the way eigenvalues are paired between $\phi = 0$ and π can never be altered, since each Kramers doublet remains stucked at $\phi = 0$ and π . In other words, it is impossible to change the topology of the ‘band-line’ continuously from the type of Fig. 2(a) to (b), without breaking the TR symmetry.

If a state is exponentially localized, its eigen energy must be insensitive to the boundary phase factor, i.e., the ‘band width’ of $E_n(\phi)$ is exponentially small compared with the average level spacing [23]. In the Dirac model, however, it is impossible because all the band lines are connected through the Kramers doublets at $\phi = 0, \pi$ so that the band width cannot be smaller than the level spacing. We thus conclude that there are no localized states in the Hamiltonian (2). In the non-relativistic electron system, in contrast, the structure of the spectrum in Fig. 2 (b) does not, at least, prohibit localization, and states indeed tend to be localized for strong disorder.

We note that, in order for the above argument to be valid, we have to assume that the energy band continues from $-\infty$ to ∞ . Indeed, if we have a finite cutoff, the TR symmetry must be broken either at $\phi = 0$ or π . Although this may alter the band-line topology around the band edges, the low-energy states around the Dirac point are hardly affected as long as the disorder potential is long-ranged and the cut-off is large enough. With increasing the disorder strength, one would naively expect Anderson localization first takes place at band edges (cut-off) and the Dirac point (can be viewed as a point at which two band edges meet accidentally). The former goes away as we send the cutoff to infinity, while the latter is protected from localization by the topology of the spectral flow.

Although the honeycomb lattice system involves a coupling of the two valleys (flavors), a similar delocalization effect should manifest itself when intervalley scattering is negligibly weak. On the other hand, when atomic-scale scatterers dominate, the intervalley scattering randomizes the Berry phase and the nature of interference is changed to enhance localization.[10] In the Dirac band, the inter-valley scattering time depends on the Fermi energy as $\propto 1/|E_F|$ [5], and thus is more important in the highly doped regime.

The present calculation suggests that the Dirac fermion system exhibits the positive magnetoresistance. On the other hand, the recent graphene experiments indicate somewhat complicated situations: A magnetoresistance study [27] clarified that highly doped epitaxial graphene exhibits a crossover between positive and negative magnetoresistance induced by changing the temperature as expected theoretically in Refs.[6, 28]. For isolated single graphene sheets[4], however, experiments show that (i) the conductivity hardly changes in a wide

range of temperature near the Dirac point, while (ii) the magnetoresistance is weakly positive at low carrier densities.[29] Although a number of theoretical scenarios have been proposed, including effects of microscopic ripples [29, 30], trigonal warping terms [28], and edges [31], there is no consensus at this moment. Taking into account these effects in addition to the random scalar potential in Eq. (2) will be done elsewhere.

Although our focus in this paper is on 2D, the argument based on the topology of the spectral flow applies equally well to the 1 and 3D two-component massless Dirac fermion with the effective TR symmetry: A two-component massless Dirac fermion cannot be localized by a random scalar potential in all 1, 2, and 3D.[32] Since d -dimensional two-component massless Dirac fermion can be viewed as a gapless boundary mode of \mathbb{Z}_2 topological insulators in $(d+1)$ D ($d = 1, 2, 3$)[7, 8, 9], our discussion above concludes that a surface of a (strong) \mathbb{Z}_2 topological insulator is always metallic, robust against disorder. This is consistent with the speculation in Ref. [7] in the context of quantum spin Hall effect. Such metallic surface states can be called a “topological metal” [7].

After completion of this work, we became aware of a similar numerical result at the Dirac point, obtained independently in Ref. [24].

The Authors acknowledge helpful interactions with A. H. Castro-Neto, L. Fu, A. Geim, A. W. W. Ludwig, A. H. MacDonald, and D. N. Sheng. K. N. and S. R. acknowledge the workshop “Electronic Properties of Graphene” at the Kavli Institute for Theoretical Physics at Santa Barbara, where this work was initiated. This work was supported by the National Science Foundation under Grant No. PHY05-51164.

-
- [1] E. Abrahams, P. W. Anderson, D. C. Licciardello, and T. V. Ramakrishnan, *Phys. Rev. Lett.* **42**, 673 (1979).
- [2] An exception to the single parameter scaling is the two parameter scaling of the integer quantum Hall effect: D. E. Khmel'nitskii, *JETP Lett.* **38**, 552 (1983); A. M. M. Pruisken, *Nucl. Phys. B* **235**, 277 (1984).
- [3] Patrick A. Lee and T. V. Ramakrishnan, *Rev. Mod. Phys.* **57**, 287 (1985).
- [4] K. S. Novoselov, A. K. Geim, S. V. Morozov, D. Jiang, Y. Zhang, S. V. Dubonos, I. V. Grigorieva, and A. A. Firsov, *Science* **306**, 666 (2004).
- [5] H. H. Shon and T. Ando, *J. Phys. Soc. Jpn.* **67**, 2421 (1998).
- [6] T. Ando and H. Suzuura, *J. Phys. Soc. Jpn.* **71**, 2753 (2002); H. Suzuura and T. Ando, *Phys. Rev. Lett.* **89**, 266603 (2002).
- [7] L. Fu, C. L. Kane, and E. J. Mele, *Phys. Rev. Lett.* **98**, 106803 (2007); L. Fu and C. L. Kane, *Phys. Rev. B* **76**, 045302 (2007).
- [8] J. E. Moore and L. Balents, *Phys. Rev. B* **75**, 121306(R) (2007).
- [9] R. Roy, *cond-mat/0607531* (unpublished).
- [10] T. Ando and T. Nakanishi, *J. Phys. Soc. Jpn.* **67**, 1704 (1998); T. Ando, T. Nakanishi, and R. Saito, *ibid.*, 2857 (1998).
- [11] A. W. W. Ludwig, M. P. A. Fisher, R. Shankar, and G. Grinstein, *Phys. Rev. B* **50**, 7526 (1994).
- [12] S. Hikami, A. I. Larkin, and Y. Nagaoka, *Prog. Theor. Phys.* **63**, 707 (1980).
- [13] Y. Asada, K. Slevin, and T. Ohtsuki, *Phys. Rev. B* **70**, 035115 (2004).
- [14] P. Markos and L. Schweitzer, *J. Phys. A: Math. Gen.* **39**, 3221 (2006).
- [15] S.-H. Dong, X.-W. Hou, and Z.-Q. Ma, *Phys. Rev. A* **58**, 2160 (1998).
- [16] M. I. Katsnelson, K. S. Novoselov, and A. K. Geim, *Nature Phys.* **2**, 620 (2006).
- [17] P. Fendley, *Phys. Rev. B* **63**, 104429 (2001).
- [18] P. M. Ostrovsky, I. V. Gornyi, and A. D. Mirlin, *Phys. Rev. Lett.* **98**, 256801 (2007).
- [19] S. Ryu, C. Mudry, H. Obuse, and A. Furusaki, *cond-mat/0702529* (unpublished).
- [20] K. Nomura and A. H. MacDonald, *Phys. Rev. Lett.* **98**, 076602 (2007).
- [21] A. Rycerz, J. Tworzydło, and C. W. J. Beenakker, *cond-mat/0612446* (unpublished).
- [22] T. Ando, *J. Phys. Soc. Jpn.* **52**, 1740 (1983); **53** 3101 (1984); **53** 3126 (1984).
- [23] D. J. Thouless and S. Kirkpatrick, *J. Phys. C* **14**, 235 (1981); Y. Imry, *Introduction to Mesoscopic Physics*, Oxford University Press (1997).
- [24] For a careful discussion on the single parameter scaling at the Dirac point, see J. H. Bardarson, J. Tworzydło, P. W. Brouwer, and C. W. J. Beenakker, *arXiv:0705.0886* (unpublished).
- [25] Our numerical beta function indicates that the phase diagram obtained for the disordered quantum spin Hall system by H. Obuse, A. Furusaki, S. Ryu, and C. Mudry, *Phys. Rev. B* **76**, 075301 (2007), and by A. M. Essin and J. E. Moore, *arXiv:0705.0172* (unpublished), is a generic one. In other word, whenever two different 2D \mathbb{Z}_2 insulators are connected by a insulator-insulator transition, it should be described by the universality class of the integer quantum Hall effect.
- [26] A similar switching of Kramers pairs was found in the position of the Wannier states in the \mathbb{Z}_2 pumping, L. Fu and C. L. Kane, *Phys. Rev. B* **74**, 195312 (2006).
- [27] Xiaosong Wu, Xuebin Li, Zhimin Song, Claire Berger, and Walt A. de Heer, *Phys. Rev. Lett.* **98**, 136801 (2007).
- [28] E. McCann, K. Kechedzhi, Vladimir I. Falko, H. Suzuura, T. Ando, and B. L. Altshuler, *Phys. Rev. Lett.* **97**, 146805 (2006).
- [29] S. V. Morozov, K. S. Novoselov, M. I. Katsnelson, F. Schedin, L. A. Ponomarenko, D. Jiang, and A. K. Geim, *Phys. Rev. Lett.* **97**, 016801 (2006).
- [30] A. F. Morpurgo and F. Guinea, *Phys. Rev. Lett.* **97**, 196804 (2006).
- [31] E. Louis, J. A. Verges, F. Guinea, and G. Chiappe, *Phys. Rev. B* **75**, 113407 (2007).
- [32] From the field theory point of view, the topological term in the NL σ M is responsible for the delocalization in 1 and 2D. The 3D NL σ M for the symplectic symmetry class does not allow topological terms, but a Chern-Simons type term is possible, which might be responsible for the delocalization. See for example, A. G. Abanov, *Phys. Lett. B* **492**, 321 (2000).